論文 한국정밀공학회지 제10권 제4호 1993.12
Journal of the Korean Society of Precision Engineering Vol. 10. No.4 Dec. 1993.

로봇의 정밀도 향상을 위한 평행식 구조의 정밀로봇 설계

한 창 수*

The Optimum Design of A 6 D.O.F Fully-Parallel Micromanipulator for Enhanced Robot Accuracy

Chang-Soo Han*

ABSTRACT

이 논문에서는 정밀로봇 설계에 관한 여러 사안을 다루었다. 정밀로봇이란 미세한 오차와 정밀한 제어로 기존 로봇의 정밀도 향상을 위한 작고, 정밀한 운동범위를 갖춘 로봇이다. 원하는 운동범위나 효과적인 힘 전달률, 최소한 작은 힘으로의 동작을 수행하기 위한 최적의 기구학적 변수를 컴퓨터 시뮬레이션을 통하여 구현하고자 한다. CAD/CAM 시스템을 이용한 합성, 해석 및 제작을 위한 정보가 만들어질 수 있으며 최대 휨 및 응력해석을 통하여 최종적인 검증 및 설계 변경을 위한 자료로서 사용될 수 있을 것이다.

Key Words : Parallel(평행식 구조), Micromanipulator(정밀로봇), Robot Accuracy(로봇정밀도), Analysis (해석), Synthesis(합성)

1. INTRODUCTION

The idea behind the Stewart platform(1) type of micromanipulator (Fig. 1) is to design and build a small amplitude, high resolution parallel mechanism which vields high structural rigidity and balanced load distributions as compared to a serial mechanism.

The resulting compact small device can be mounted on any existing macro robot between the wrist and end effector to provide fine adjustments for precise error compensation and delicate force contol through general spatial 6 D.O.F motion. Therefore, the proposed system will superimpose high resolution micromanipulator control over the large motion range of macromanipulator module.

Thus, it permits not only real time compensation for high speed but also very accurate positioning for fine motion. The actuators of the large robot could be specially designed for high speed and flexibility, while the micromanipulator actuators would be specially designed for accurate fine motion. Conventional robots have two major limitations, lack of speed and positioning errors.

No robot is precise under large payload or at high speeds. If a robot is made stiffer for

* 한양대학교 기계공학과

increased accuracy, speed is usually inversely affected. Limited accuracy is due to inertia effects, static friction and backlash in the joint, link bending deflections, and finite encoder resolution, etc.

Most industrial robots have been designed to carry large payloads in a relatively large workspace and their weight, size, and cost is also usually large. As a result, the resolution is not fine enough for high precision tasks which require positional error compersation at scales mach smaller than the coarse resolution of the robot. In addition, robots do not operate in terms of a real time dynamic model to compernsate for deformations resulting from external loads.

Since the large robot system is highly nonlinear, its operation would be difficult to treat dynamically in real time. However, due to the small motion range of the proposed micromanipulator system, it is highly linear and can easily compensate for system inaccuracies in real time.

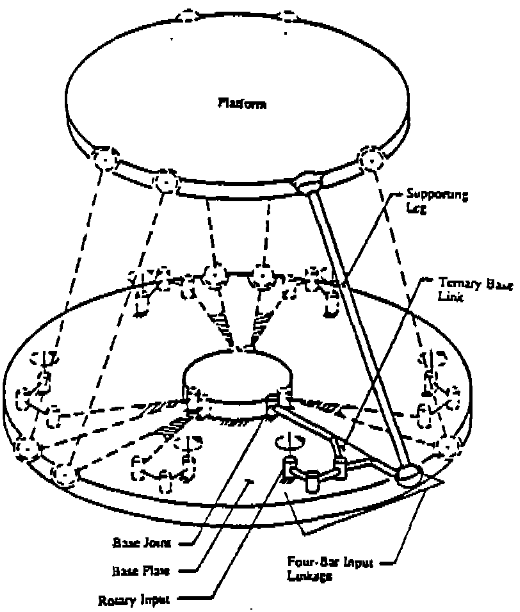

Fig. 1 Kinematic representation of the micromanipuator

This means that the large motion could be compensated for by the small scale motion of the micromanipulator module.

2. DESIGN OBJECTIVES

As robotic functions become more and more complicated, and the range of applications is widened, optimal robot designs will be needed to minimize cost while maximizing performance. The design process seeks to define the basic parameters of the robot which are more of less closely associated with the mechanical structure. Those parameter to be considered are payload, mobility, workspace, compactness, repeatability, accuracy, agility, structural stiffness, damping coefficients, natural frequencies, and finally, economic factors like cost, reliability, maintainability, etc. The detailed design specifications were developed for the design of a micromanipulator.

- 6 D.O.F motion
- Payload capacity(10 lb to 100 lb)
- Motion range(+0.1″ to -0.1″, +2 degree to -2 degree)
- Size(depends on end effector diameter)
- High resolution(1 part in 1000)
- Bandwidth(greater than 50 HZ)
- No backlash
- Minimal friction
- Minimum weight
- Compactness
- Linearity
- Repeatability
- Rigidity

3. MODEL REPRESENTATION AND PARAMETERS

3.1 Kinematic model description of upper structure

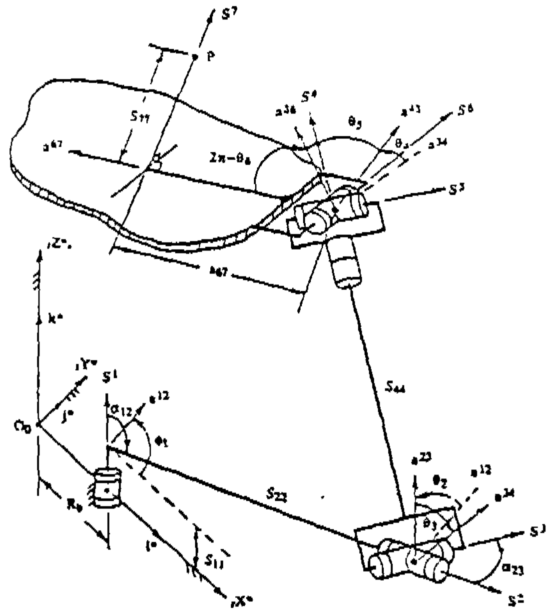

Fig. 2 Kinematic representation of upper structure

3.2 Kinematic model description of lower 4 bar linkage

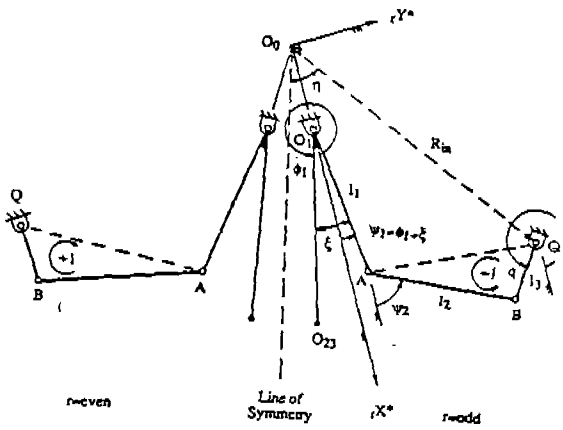

Fig. 3 Kinematic representation of lower 4 bar linkage

3.3 Parameters to be optimized

Link dimensions :

$S_{11}=0$ (inches)

S_{22}=normalized reference value

S_{44}=supporting leg

$S_{77}=0$

L_1=output link 4 bar

L_2=coupler link in 4 bar

L_3=input link 4 bar

Angular parameters [degrees]

λ_0=base joint connection angle

γ_0=platform connection angle

ξ=4 bar linkage angle

ζ=motor position angle

Radial parameters [inches]

R_p=radius of the platrorm (inches)

R_b=radius of the base

R_{in}=radius of the motor position

4. DESIGN PROCESS

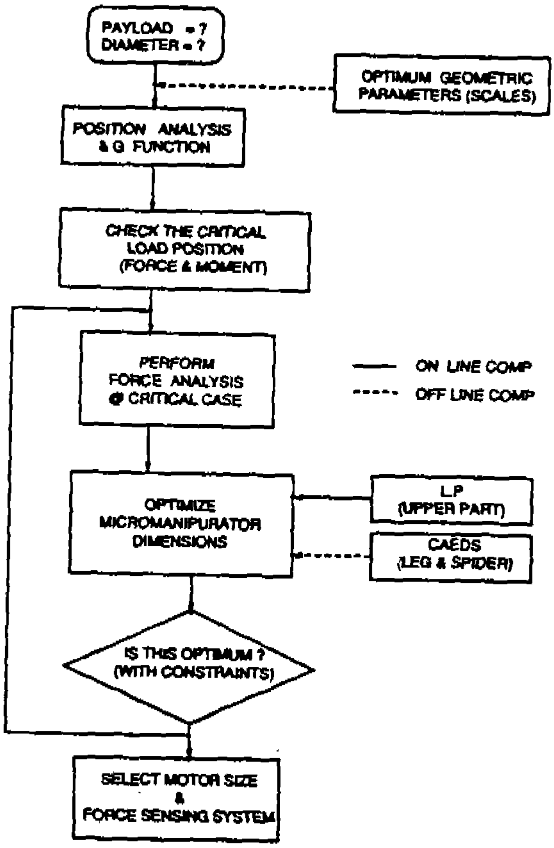

Fig. 4 Flowchart of the design process

The flowchart of the design process shown in Figure. 4 includes the systematic steps needed to determine the optimal system geometry and dimensions of the detailed hardware design required for performing a given task. The goal is to use powerful design tools which address local and global design issues.

4.1 Kinematic & dynamic modeling analysis

The fundamental concepts in the general kinematic and dynamic model formulation are the Kinematic Influence Coefficient (KIC) [2, 3] and the generalized coordinate transformation [4]. The idea of KIC is based on the separation of time dependent and position dependent functions. Further developments extended this approach to the analysis of serial manipulators [5, 6], and hybrid parallel/serial manipulators [7].

Feasibility study of a platform type of robotic manipulator from a kinematic viewpoint has been performed [8, 9]. With the use of these ideas, a kinematic and dynamic model formulation referenced to the actuator coordinates for the fully parallel 6 D. O. F micromanipulator and a kinematic rapresentations of this mechanism are represented in the literature [10]. This analytical foundation will guide the design, manufacture, implementation, and control [11, 12] of this unique micromanipulator. The computer simulation based on these kinematic and dynamic modeling formulations will be used to determine optimal geometry for the micromanipulator. The author will briefly mention the basic kinematic and dynamic equations required in the modeling.

Using the chain rule, the first order time derivative of $\underline{u}$ is

$$\frac{d\underline{u}}{dt}=\frac{\partial \underline{u}}{\partial \underline{\varphi}}\frac{\partial \underline{\varphi}}{\partial t} = \frac{\partial \underline{u}}{\partial \underline{\varphi}}\dot{\underline{\varphi}} \qquad (4.1.1)$$

By defining the first and second order kinematic influence coefficients, which will be referred to as the G-function and H-function respectively, as

$$\left[G^{u}_{\bullet}\right]=\frac{\partial \underline{u}}{\partial \underline{\varphi}} \quad \left[H^{u}_{\bullet\bullet}\right]=\left(\frac{\partial}{\partial \underline{\varphi}}\left[G^{u}_{\bullet}\right]\right)=\left(\frac{\partial}{\partial \underline{\varphi}}\frac{\partial \underline{u}}{\partial \underline{\varphi}}\right) \qquad (4.1.2)$$

then

$$\dot{\underline{u}}=\left[G^{u}_{\bullet}\right]\dot{\underline{\varphi}} \qquad (4.1.3)$$

and

$$\ddot{\underline{u}}=\left[G^{u}_{\bullet}\right]\ddot{\underline{\varphi}}+\dot{\underline{\varphi}}^{T}\left[H^{u}_{\bullet\bullet}\right]\dot{\underline{\varphi}} \qquad (4.1.4)$$

The dynamic equation is derived from the principles of virtual work and d'Alembert with previously obtained kinematic influence coefficient.

$$\underline{T}^{L}_{\bullet}=\sum_{j=1}^{M}\left\{\left[{}^{j}G^{p}_{\bullet}\right]^{T}{}^{j}\underline{f}^{p}+\left[G^{jk}_{\bullet}\right]^{T}\underline{m}^{jk}\right\} \qquad (4.1.5)$$

where $\underline{T}^{L}_{\bullet}$ is defined as the effective input loads.

The effective inertial load is

$$\underline{T}^{I}_{\bullet}=\left[I^{*}_{\bullet\bullet}\right]\ddot{\underline{\varphi}}+\dot{\underline{\varphi}}^{T}\left[P^{*}_{\bullet\bullet\bullet}\right]\dot{\underline{\varphi}} \qquad (4.1.6)$$

where

$$\left[I^{*}_{\bullet\bullet}\right]=\sum_{j=1}^{M}\left\{M_{jk}\left[{}^{j}G^{c}_{\bullet}\right]^{T}\left[{}^{j}G^{c}_{\bullet}\right]+\left[G^{jk}_{\bullet}\right]^{T}\left[\Pi^{jk}\right]\left[G^{jk}_{\bullet}\right]\right\}$$

and

$$\left[P^{*}_{\bullet\bullet\bullet}\right]=\sum_{j=1}^{M}\left\{M_{jk}\left[{}^{j}G^{c}_{\bullet}\right]^{T}\cdot\left[{}^{j}H^{c}_{\bullet\bullet}\right]+\left[G^{jk}_{\bullet}\right]^{T}\left[\Pi^{jk}\right]\cdot\left[H^{jk}_{\bullet\bullet}\right]+\left[G^{jk}_{\bullet}\right]^{T}\left(\left[G^{jk}_{\bullet}\right]^{T}\cdot\left[\Xi^{jk}\right]\right)\left[G^{jk}_{\bullet}\right]\right\}$$

Having determined the equations for the applied and effective intertial loads, the general dynamic equation can be expressed as

$$
\begin{aligned}
\mathrm{I}_{\phi} &= \mathrm{I}^{I}_{\phi} - \mathrm{I}^{L}_{\phi} \\
&= \left[\mathrm{I}^{*}_{\phi\phi}\right]\ddot{\underline{\varphi}} + \dot{\underline{\varphi}}^{T}\left[\mathrm{P}^{*}_{\phi\phi\phi}\right]\dot{\underline{\varphi}} \\
&- \sum_{j=1}^{M}\left\{\left[{}^{j}\mathrm{G}^{p}_{\phi}\right]^{T}{}^{j}\mathbf{f}^{p} + \left[\mathrm{G}^{jk}_{\phi}\right]^{T}\mathbf{m}^{jk}\right\}
\end{aligned}
\qquad (4.1.7)
$$

4.2 Find optimum geometric parameters

First, one needs to fully understand how the basic parameters affect the motion range[13, 14, 15], transmission ratio[16], manipulability[17], dexterity[18], singularity, and agility. By using computer simulation based on the kinematic and dynamic formulations, one can determine specifications of the optimal system geometry satisfying a set of design objectives. Possible design objectives are; desired motion range, effective force and velocity transmission ratio, joint bending load, dexterity, agility, manipulability, and minimal variations in the elements of the modeling coefficients. There are 14 parameters to be optimized for this mechanism. The basic idea behind this is the generalized eigenvalue analysis (Appendix) of the system Jacobian matrix. These concepts are applied to set up optimal system geometry parameters for the micromanipulator by finding the maximum and minimum bounds of the transmission ratio[19]. Secondly, to maximize the motion range of the platform, one needs to synthesize the optimum 4 bar linkage considering the input and output angle ratio of this mechanism. A design tool has been developed and applied in a synthesis of the 4 bar linkage mechanism subject to constraints. The optimum set of geometric parameters and joint angle have been identified.

4.3 Force analysis

The objectives of the force analysis are to determine the required input, constraint reaction forces, the internal stresses in components, bearing loads, and evalulation of the deformation in critical members of the system. A clear understanding of the forces acting in the system allows the designer to create an optimum shape of the components as well as to select appropriate materials and dimensions of those members to comply with the performance specifications. To do this, the module is divided into two parts which are the upper structure and the lower 4bar linkage.

A. Upper structure

The difficulty of force analysis of the Stewart type parallel mechanism is to solve the constraint reaction of the six legs, which connect the platform and base. We can assume the moment components are zero and consider only three unknown force components. This means that the axial load computed are sufficient to support the static applied loads and main source of loading (Fig. 5). This assumption is compatible with the physical reality of a relatively small servo motor and a close fit between the crank

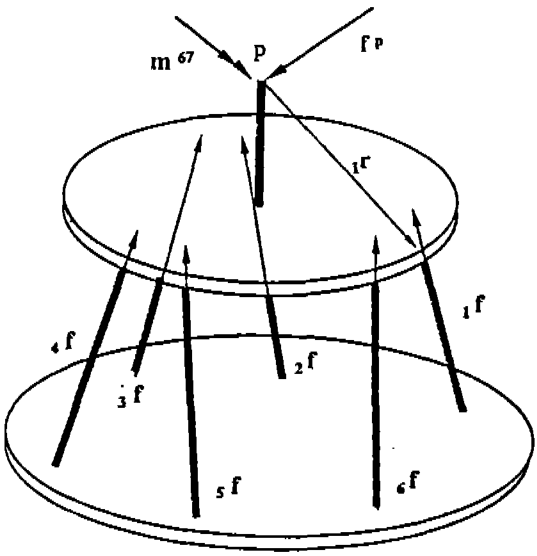

Fig. 5 Load vector applied to the platform

ends and the stiff base plates.

(i). $\sum F = 0$

$${}_r f^4 = {}_r f\, {}_r s^4 \qquad ; r = 1,2,....6$$

$$F^p = \sum_{r=1}^{6} {}_r f^4\, {}_r s^4$$

$$F^p = \left[{}_1 s^4\ {}_2 s^4\ {}_3 s^4\ \cdots {}_6 s^4 \right] \begin{Bmatrix} {}_1 f^4 \\ {}_2 f^4 \\ \vdots \\ {}_6 f^4 \end{Bmatrix} \tag{4.3.1}$$

(ii). $\sum M = 0$

$$\begin{aligned} {}_r m^{67} &= {}_r r \times {}_r f^4 \\ &= -(a_{67}\, {}_r a^{67} + s_{77} k) \times {}_r f^4 \\ &= {}_r s^4 \times (a_{67}\, {}_r a^{67} + s_{77} k)\, ({}_r f^4) \end{aligned}$$

$$M^{67} = \sum_{r=1}^{6} {}_r s^4 \times (a_{67}\, {}_r a^{67} + s_{77} k)\, ({}_r f^4)$$

$$M^{67} = \left[{}_1 s^4 \times {}_1 r \mid {}_2 s^4 \times {}_2 r \mid \cdots \mid {}_6 s^4 \times {}_6 r \right] \begin{Bmatrix} {}_1 f^4 \\ {}_2 f^4 \\ \vdots \\ {}_6 f^4 \end{Bmatrix} \tag{4.3.2}$$

$$\begin{Bmatrix} F^p \\ M^{67} \end{Bmatrix} = \begin{bmatrix} {}_1 s^4 & | & {}_2 s^4 & | & \cdots | & {}_6 s^4 \\ {}_1 s^4 \times {}_1 r & | & {}_2 s^4 \times {}_2 r & | & \cdots | & {}_6 s^4 \times {}_6 r \end{bmatrix} \begin{Bmatrix} {}_1 f^4 \\ {}_2 f^4 \\ \vdots \\ {}_6 f^4 \end{Bmatrix} \tag{4.3.3}$$

$$\begin{Bmatrix} {}_1 f^4 \\ {}_2 f^4 \\ \vdots \\ {}_6 f^4 \end{Bmatrix} = \begin{bmatrix} {}_1 s^4 & | & {}_2 s^4 & | & \cdots | & {}_6 s^4 \\ {}_1 s^4 \times {}_1 r & | & {}_2 s^4 \times {}_2 r & | & \cdots | & {}_6 s^4 \times {}_6 r \end{bmatrix}^{-1} \begin{Bmatrix} F^p \\ M^{67} \end{Bmatrix} \tag{4.3.4}$$

B. Lower four bar linkage

From previous force analysis of the leg in the upper structure, one can calculate the unknown reaction forces to establish the force balance. That reaction force is directly related to the required input torque at the motor. The force transmitted from the leg is decomposed into vertical and horizontal components. The horizontal force component is equivalent to the external force and 6 unknown forces at the link joint as well as required torque input can be obtained by solving 6 linear equations.

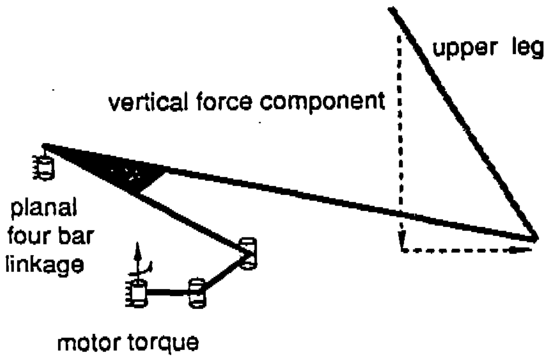

Fig. 6 Force vector applied to the 4 bar linkge

4.4 Fiexural member disign

A. Optimum dimension of component

Special attention must paid to design critical flexural components to have low stiffness, low inertia, and no backlash while maintaining a structurally sound system. Here, the concept is to determine and optimize the dimensions of the necked down flexural joint part for specified deflection and predetermined link length is described. The flexural hinge to be designed is shown in the Figure. 7

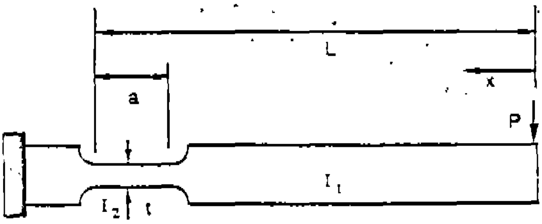

Fig. 7 Flexural joint

The member consists of a beam of lengh 'L' in which a portion (length 'a') has a reduced cross section. The portion of the member between the load and the hinge has a moment of inertia I_1, which is much larger than the moment of inertia I_2 of the hinge portion of the beam. It is required to find the deflection of the end of the beam under load P.

Castigliano's theorem will be used to determine the deflection for the pure bending stress, the theorem stated as follows :

$$\delta = \int_0^L \frac{M}{EI}\frac{\partial M}{\partial P}dx \tag{4.4.1}$$

The bending moment M is given by

$$M = PX \tag{4.4.2}$$

So,

$$\delta = \int_0^{L-a} \frac{M}{EI_1}\frac{\partial M}{\partial P}dx + \int_{L-a}^{L} \frac{M}{EI_2}\frac{\partial M}{\partial P}dx$$

$$= \int_{L-a}^{L} \frac{M}{EI_2}\frac{\partial M}{\partial P}dx \qquad \text{, with } I_1 >> I_2$$

$$= \int_{L-a}^{L} \frac{PX^2}{EI_2}dx$$

$$= \left[\frac{PX^3}{3EI_2}\right]_{L-a}^{L} = \frac{P}{3EI_2}\left[L^3 - (L-a)^3\right]$$

$$= \frac{P}{3EI_2}\left[3L^2a - 3a^2L + a^3\right] \tag{4.4.3}$$

The stress in the flexural hinge can be determined from the flexure formula :

$$\sigma = \frac{Mc}{I_2}$$

$$\sigma_{max} = \frac{PLc}{I_2} = \frac{PLt}{2I_2}, \quad I_2 = \frac{PLc}{\sigma} = \frac{PLt}{2\sigma}$$

$$\text{where} \quad M = PL,\ c = t/2 \tag{4.4.4}$$

Substitute this equation into the deflection equation to yield :

$$\delta = \frac{2\sigma}{3ELt}(3L^2a - 3a^2L + a^3) \tag{4.4.5}$$

To put in dimensionless form, divie both sides by L.

$$\frac{\delta}{L} = 2\left(\frac{\sigma}{E}\right)\left[\frac{a}{t} - \left(\frac{a}{L}\right)\left(\frac{a}{t}\right) + \frac{1}{3}\left(\frac{a}{L}\right)^2\left(\frac{a}{t}\right)\right]$$

$$\frac{\delta}{L} = 2\left(\frac{\sigma}{E}\right)\left(\frac{a}{t}\right)\left[1 - \left(\frac{a}{L}\right) + \frac{1}{3}\left(\frac{a}{L}\right)^2\right] \tag{4.4.6}$$

This dimemsionless form allows us to plot contours for determining link dimensions for specified deflections and L. Therefore, this equation gives δ/L as a function of a/t and a/L for any constant value of $\sigma/E = 0.001$. Figure. 8 shows the chart for determining link dimensions.

For instance,

for steel, $E = 30 \times 10^6$ psi (Young's modulus)

$\sigma = 30,000$ psi (strength)

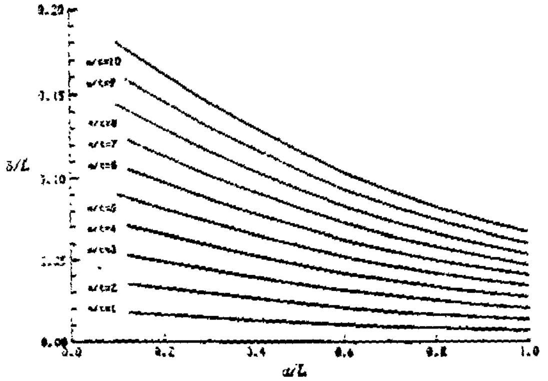

Fig. 8 Chart for determining link dimensions

Given $\delta = 0.1''$, we can calculate δ/L. There we can choose various a/L resulting in different a/t's from chart. This allows us to choose a particular thickness t for the given parameters.

B. Optimum cross section by Linear Programming

By finding the optimum cross section of the legs, we can minimize total weight, minimize inertial effects, and increase the payload. Optimizaion is carried out by using linear programming[20] under the design constraints which are displacement limitations, allowable axial stress in leg, avoid buckling, and positive cross section area.

i, e Minimize objective function

$$Z = \text{TOTAL WEIGHT} = F(X) \qquad (4.4.7)$$

Subject to design contraints

$$G_j \geq 0 \quad j = 1,2,\ldots m$$

m=number of constraints

x=cross section area

OBJECTIVE FUNCTION

MINIMIZE:

$$\sum_{i=1}^{m} \rho_i L_i X_i$$

CONSTRAINTS.

$$\sum_{i=1}^{n} \frac{P_{ij} L_i}{E_i X_i} \leq \delta_{jk} \qquad \text{displacement limitation}$$

$$\overline{\sigma_{si}} \leq \frac{P_{ij}}{X_i} \leq \sigma_{si} \qquad \text{axial stress}$$

$$\overline{\sigma_{bi}} \leq \frac{\pi^2 E_i I_i}{L_i^2 X_i} \qquad \text{buckling stress}$$

$$\overline{X_i} \leq X_i$$

4.5 Finite element application for analysis

Final checking or modification to insure meeting the design criteria is made based on the local maximum stress and deflection analysis. The component models are analyzed using Computer Aided Engineering Design System (CAEDS) which is an integrated finite element solver, composed of the finite element analysis package and pre, post prosessing package*. Here, the two important parts in the micromanipulator design, the supporting leg (Fig. 9-12) and the planar four bar input linkage mechanism (Fig. 13-16) are analyzed. The results of the components analysis can then be interactively displayed using the Graphics system serving as a postporsessor.

5. CONCLUSION

The idea of the simulation, computer aided design, optimization theory, and finite element method is being used in designing the 6 D. O. F. fully parallel micromanipulator robot. Design objectives and the detailed design process which shows the systematic steps needed to determine the optimal system geometry and dimensions of the components to comply with

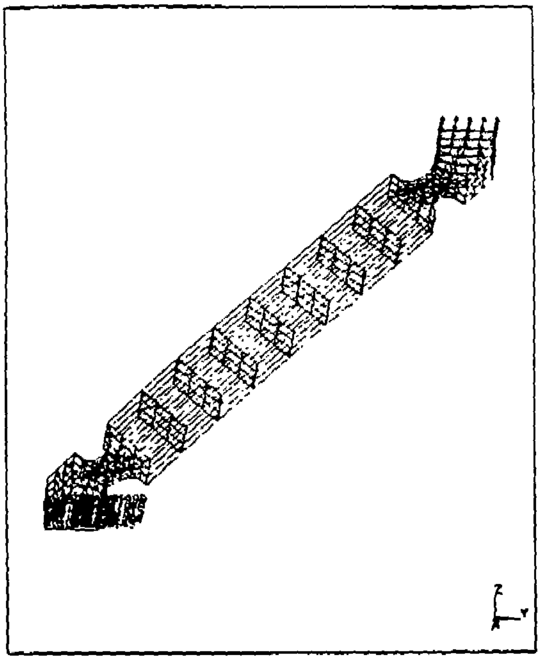

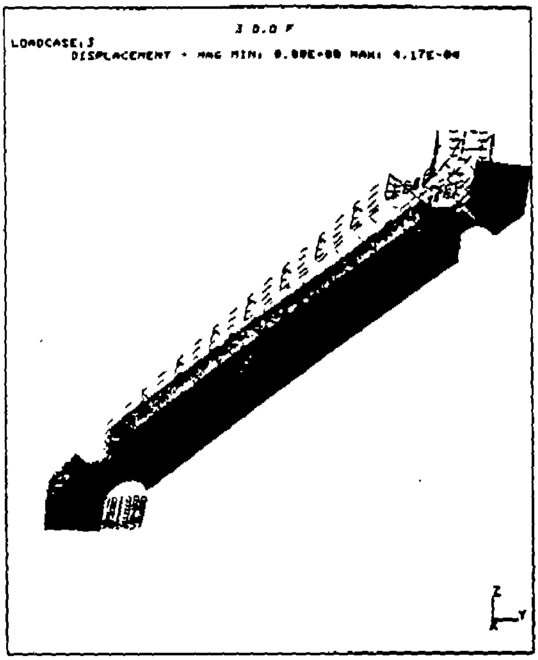

Fig. 9 Finite element model developed with CAEDS

Fig. 10 Deflection analysis of the leg

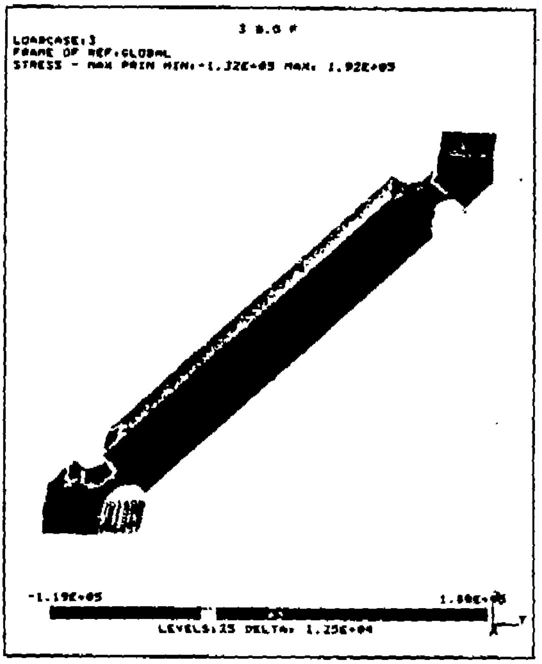

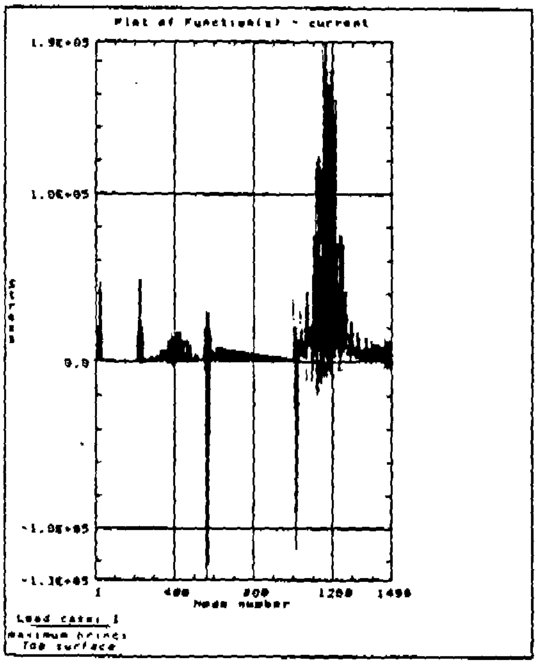

Fig. 11 Element stress analysis of the leg

Fig. 12 Node stress analysis of the leg

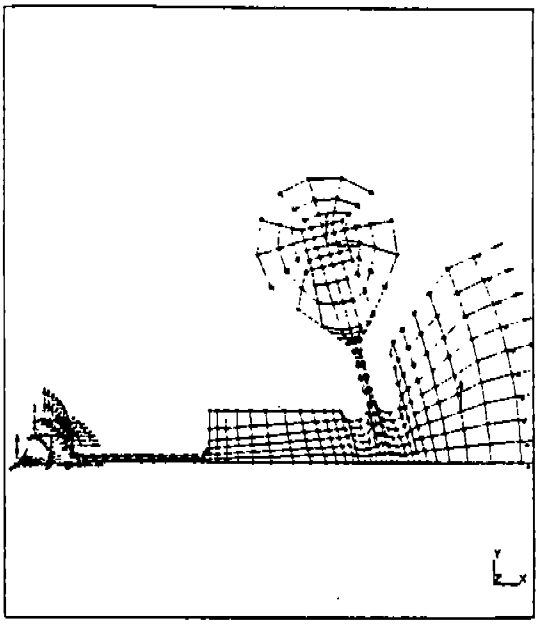

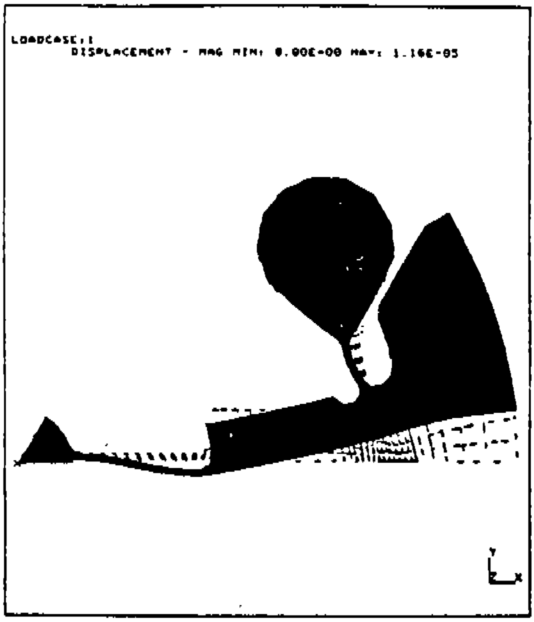

Fig. 13 Finite element model developed with CAEDS

Fig. 14 Deflection analysis of the 4 bar link

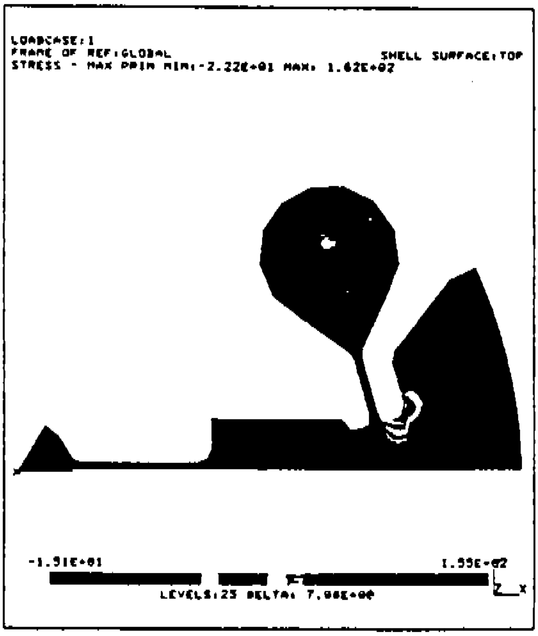

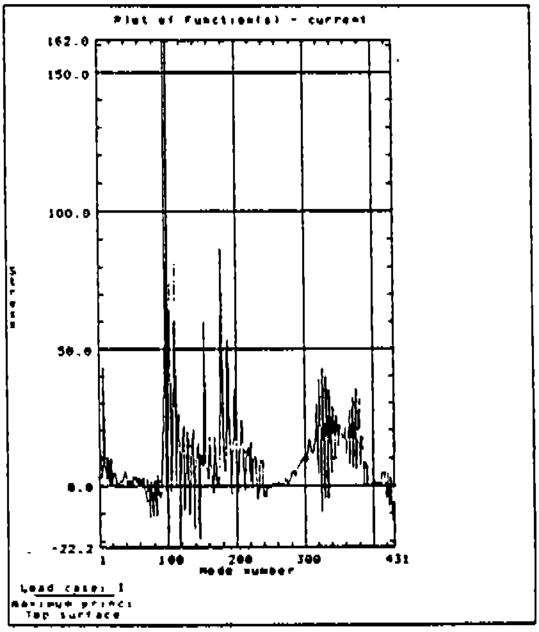

Fig. 15 Element stress analysis of the 4 bar link

Fig. 16 Node stress analysis of the 4 bar link performance specifications are analyzed. The use of those integrated tools permits an increase in the productivity of the designer and a more through engineering analysis.

Appendix

It is useful to define the ratio of the Euclidean norm (vector 2 norm) of the generalized input load to that of a generalized output load.

$$\tau = \frac{\|T_i\|}{\|T_o\|} \qquad (a.1)$$

then,

$$\|T_i\| = (T_i^T T_i)^{1/2}$$

$$\|T_o\| = (T_o^T T_o)^{1/2}$$

$$T_i = [G]^T T_o .$$

Therefore,

$$\tau = \left[\frac{T_i^T T_i}{T_o^T T_o}\right]^{1/2} = \left[\frac{T_o^T[G]\,[G]^T T_o}{T_o^T T_o}\right]^{1/2} \qquad (a.2)$$

The expression inside the squrare root is known as the Rayleigh quotient(19), i.e. the eigenvalues λ of the matrix product$[G][G]^T$ can be used to describe the global condition of the system. Then, the ratio of the vector 2 norm of the input to output load is bounded by the square root of λ_{min} and λ_{max},

$$(\lambda_{min})^{1/2} \le \frac{\|T_i\|}{\|T_o\|} \le (\lambda_{max})^{1/2} \qquad (a.3)$$

$$\|T_o\|\,(\lambda_{min})^{1/2} \le \|T_i\| \le \|T_o\|\,(\lambda_{max})^{1/2} . \qquad (a.4)$$

An analogous result can be derived for velocity using the fact that $[G][G]^T$ is symmetric. But there is a contradiction not only between force and velocity from the compatibility point of view, but also between respective magnitudes from the control point of view. Awareness of this contradiction allows the designer to make a satisfactory balance or tradeoff between these two values.

ACKNOWLEDGEMENT

The author would like to express his appreciation to the Korea Science and Enginering Foundation for Supporting this research. (KOSEF)

REFERENCES

1. Stewart, D., "A Platform with Six Degrees of Freedom", proc. Institution of Mechanical Engineers, Vol. 180, Part I, No. 15, 1965-66, pp. 371~386.
2. Benedict, C. E. and Tesar, D., "Model Formulation of Complex Mechanisms with Multiple Inputs : Part I Geometry", ASME Journal of Mechanical Design, Vol. 100, October 1978a, pp. 747~753.
3. Benedict, C. E. and Tesar, D., "Model Formulation of Complex Mechanisms with Multiple Inputs : Part II, The Dynamic Model", ASME Journal of Mechanical Design, Vol. 100, October 1978b, pp. 755~761.
4. Freeman, R. A. and Tesar, D., "The Generalized Coordinate Selection for the Dynamics of Complex Planar Mechanical Systems", ASME Journal of Mechanical Design, Vol. 104, Jan. 1982, pp. 206~217.
5. Thomas, M. and Tesar, D., "Dynamic Modeling and Analysis of Rigid Link Serial Manipulators", DOE Grant DE-AC05-79ER10013. Center for Intelligent Machines and Robotics, University of Florida,

Gainesville, FL, Nov. 1982a.

6. Thomas, M. and Tesar, D., "Dynamic Modeling of Serial Manipulator Arms", ASME Journal of Dynamic Systems, Measurement, and Control, Vol. 104, Sept. 1982b, pp. 218~228.
7. Sklar, M. S. and Tesar, D., "Dynamic Analysis of Hybrid Serial Manipulator Systems Containing Parallel Modules", ASME Journal of Mechanisms, Transmissions, and Automation in Design, 1986.
8. Yang, D. H. C. and Lee, T. W., "Feasibility Study of a Platform Type of Robotic Manipulators form a Kinematic Viewpoint", ASME Journal of Mechanisms, Transmissions and Automation in Design, Vol. 106, June 1984, pp. 191~198.
9. Fichter, E. F., "A Stewart Platform Based Manipulator : General Theory and Practical Construction", The International Journal of Robotics Research, Vol. 5, No. 2, Summer, 1986.
10. Hudgens, J. and Tesar, D., "A Fully Parallel Six Degree-of-Freedom Micromanipulator : Kinematic Analysis and Dynamic Model", 20th Biennial ASME Mechanisms Conference, Kissimmee, Florida. September 25-28, 1988.
11. Sharon, A. and Hardt, D., "Enhancement of Robot Accuracy Using Endpoint Feedback and a Macro-Micro Manipulator System", American Control Conference Proc., San Diego, CA, June 6-8, 1984, pp. 1836~1842.
12. Sharon, A. and Hogan, N., and Hardt, D. E., "High Bandwidth Force Regulation and Inertia Reduction Using a macro/micro manipulator System", Proc. IEEE Int. Conference on Robotics and Automation, Philadelphia, PA. 1988, pp. 126~132.
13. Kumar, A. and Waldron, K. J., "The Dextrous Workspace", ASME paper No. 80-DET-108, 1980.
14. Bajpai, A. and Roth, B., "Workspace and Mobility of a Closed Loop Manipulator", The International Journal of Robotics Research, Vol. 5, No. 2, Summer, 1986.
15. Gupta, K. C. and Roth, B., "Design Considerations for Manipulator Workspace", ASME Journal of Mechanical Design. Vol. 104, October, 1982.
16. Chiu, S. L., "Kinematic Characterization of Manipulators : An Approach to Defining Optimality", Proc. IEEE Int. Conference on Robotics and Automation, Philadelphia, PA. 1988, pp. 828~833.
17. Yoshikawa, T., "Analysis and Control of robot manipulators with redundancy", Preprints 1st. International Symposium Robotics Research.
18. Klein, C. A. and Blaho, B. E., "Dexterity Measures for the Design and Control of Kinematically Redundant manipulators", The International Journal of Robotics Research. Vol. 6, No. 2, Summer, 1987.
19. Strag, G., Linear Algebra and Its Applications, Academic Press, New York, NY, 1980.
20. Dantzig, G. B., Linear Programming and Extensions, Princeton University Press, Princeton, NJ, 1963.